Curr Cardiovasc Imaging Rep (2016) 9: 9
DOI 10.1007/s12410-016-9371-3

Cardiac Positron Emission Tomography: a Clinical Perspective

Christian L. Polte[1,2,3] · **Iris Burck**[4] · **Peter Gjertsson**[5] · **Milan Lomsky**[5] · **Stephan G. Nekolla**[6] · **Eike Nagel**[3]

Published online: 6 February 2016

Abstract Cardiac positron emission tomography is a powerful, quantitative, non-invasive imaging modality, which adds valuable diagnostic and prognostic information to the clinical work-up. Myocardial perfusion and viability imaging are, as a result of continuously growing evidence, established clinical indications that may be cost-effective, due to the high diagnostic accuracy of cardiac positron emission tomography, despite high single-test costs. In the field of inflammation imaging, new indications are entering the clinical arena, which may contribute to a better diagnosis and overall patient care, as for instance in patients with cardiac sarcoidosis, prosthetic valve endocarditis and cardiac device infections. This review will discuss the individual strengths and weaknesses of cardiac positron emission tomography and, hence, the resulting clinical usefulness based on the current evidence for an individualized, patient-centered imaging approach.

Keywords Positron emission tomography · Myocardial perfusion · Myocardial viability · Cardiovascular inflammation · Patient-centered imaging

This article is part of the Topical Collection on *Cardiac Magnetic Resonance*

✉ Christian L. Polte
christian.polte@vgregion.se

[1] Department of Cardiology, Sahlgrenska University Hospital, 413 45 Gothenburg, Sweden

[2] Institute of Medicine, The Sahlgrenska Academy at the University of Gothenburg, Gothenburg, Sweden

[3] Institute for Experimental and Translational Cardiovascular Imaging, DZHK Centre for Cardiovascular Imaging, University Hospital Frankfurt, Frankfurt/Main, Germany

[4] Department of Diagnostic and Interventional Radiology, University Hospital Frankfurt, Frankfurt/Main, Germany

[5] Department of Clinical Physiology, Sahlgrenska University Hospital, Gothenburg, Sweden

[6] Department of Nuclear Medicine, Technical University of Munich, Munich, Germany

Introduction

Cardiac positron emission tomography (PET) is a powerful quantitative imaging modality, which enables an in-depth analysis of cardiovascular biology and physiology in health and disease. Since many years, the method has been considered as "gold standard" for perfusion and viability imaging and has, therefore, functioned as a reference standard for many other imaging modalities [1–8]. Despite its undisputed role as a high-end diagnostic and well-established research tool, cardiac PET plays still to a large extent a minor role in clinical practice. This is mainly owed to the complexity of the technique, its high costs and poorer accessibility. Nonetheless, cardiac PET is a useful and eventually even cost-effective clinical tool when used appropriately, adding valuable diagnostic and prognostic information to the diagnostic work-up [9]. In clinical practice, it is often challenging to choose from a large portfolio of competing imaging modalities, which provide frequently equivalent but sometimes also complementary information concerning a particular clinical question, as for instance in the diagnosis of stable coronary artery disease (CAD) or myocardial viability. As a sole imaging modality cannot answer every clinical question in every single patient (one-test/one-protocol approach), the final choice of imaging strategy in an individual patient should be made after a thorough consideration of the individual strengths and weaknesses/contraindications of each available, depending

on local expertise, and in the particular case useful imaging modality, with the goal to avoid layered or serial studies as well as unnecessary radiation and contrast agent exposure.

Accordingly, the aim of the current review is to provide an overview of the individual strengths and weaknesses of cardiac PET and, hence, the resulting clinical usefulness based on the current evidence for an individualized, patient-centered imaging approach.

Methodological Principles

The Physical Basis

Positron emission tomography, as the name suggests, is a tomographic imaging technique, which uses radionuclides, as for instance carbon (^{11}C), nitrogen (^{13}N), oxygen (^{15}O), rubidium (^{82}Rb), and fluorine (^{18}F), that decay by positron emission to generate an image. These radionuclides, produced in a cyclotron or an elution generator, are used to label compounds of biological interest, as for instance glucose, resulting in a so-called radionuclide-labeled tracer. Introduced in small quantities into the human body (typically 10^{13}–10^{15} molecules), the tracer is distributed throughout the body according to its biochemical properties. The subsequent beta (+) decay of the radioactive nucleus of the particularly labeled molecule results in the emission of a positron, which annihilates after a short distance (positron range) with an electron, giving rise to two annihilation 511-keV photons that travel in almost opposite directions (180° from each other) through the body until both reach the detectors surrounding the body. Importantly, only incidences of two photons arriving in opposite direction at the detector within a narrow time window of a few nano-seconds (coincidence detection) lead to an electronic signal that contributes to the final image. In the end, the image is generated after complex processing of multiple electronic signals through the application of image reconstruction and correction algorithms (correcting amongst others for attenuation, scatter, random coincidence, and dead time). In this final image, the signal from each voxel is a direct measure of the radionuclide and, hence, the labeled molecule concentration within the respective voxel, typically given in Becquerel per milliliter. Consequently, PET allows the absolute quantitative mapping of radionuclide-labeled tracers in the living human body and with the help of dynamic image sequences and compartmental modeling plus the application of operational equations even the study of tracer kinetics as well as the quantification of biological and physiological processes, as for instance myocardial blood flow (MBF) [10–12]. In recent years, several technical innovations have led to a clear improvement of image quality (improvement of image resolution and contrast as well as reduction in image noise) and reduction in radiation exposure [13–15]. Furthermore, modern PET systems usually constitute of a hybrid PET/computed tomography (CT) configuration, which use a low-dose CT scan for fast attenuation correction in contrast to the traditional transmission source-based method [16, 17].

Strengths and Weaknesses of PET in Comparison with Other Imaging Modalities

The clear strengths of cardiac PET lie, in comparison with other imaging modalities, in its high image quality, diagnostic accuracy, interpretative certainty, and ability to visualize and quantify specific biological and physiological processes. In comparison with single-photon emission computed tomography (SPECT), PET shows a superior diagnostic performance due to several reasons [18, 19]. First, PET has a better image uniformity due to well-established attenuation correction algorithms, which leads to a decrease in the number of false-positive studies and, thus, an increase in specificity. This becomes of special clinical relevance in women with large breasts and obese patients. Second, PET has a higher spatial resolution and contrast, which enables the detection of smaller defects and leads to a decrease in the number of false-negative studies and, thus, an increase in sensitivity. Third, PET has a higher temporal resolution with full and isotropic left ventricular (LV) coverage, which enables a dynamic image acquisition and thereby the assessment of LV function at peak stress, quantification of tracer kinetics, as well as the absolute quantification of regional MBF and coronary flow reserve (CFR). This is clinically of special use in patients with microvascular disease and advanced CAD with “balanced ischemia.” Fourth, PET has a higher detection sensitivity, which enables the detection of labeled molecules in extremely small quantities, namely in nano- and picomolar concentrations. In combination with the shorter half-lives of PET tracers, which enable briefer scan protocol durations and repeated studies, this leads to a reduction in the overall radiation exposure. Finally, it should be mentioned that PET tracers exhibit in general better biological and physiological characteristics than SPECT tracers. In comparison with echocardiography, cardiac CT and cardiac magnetic resonance (CMR), PET has a clear image contrast due to a high tracer versus low background signal (“hotspot imaging”), nonetheless, not in the sense of a classic soft tissue contrast, as well as a lower spatial and temporal resolution.

On the other hand, the clear weaknesses of cardiac PET lie, in comparison with other imaging modalities, in its overall poorer accessibility, methodological complexity, high costs, and radiation exposure (as SPECT and cardiac CT).

Radiopharmaceuticals for Cardiac Imaging

An overview of the currently applicable cardiac PET tracers for clinical practice and their characteristics is given in Table 1.

Table 1 Characteristics of clinically available cardiac PET tracers

Tracer	Indication	Half-life	Positron range	Myocardial uptake mechanism	First-pass extraction
^{13}N-ammonia	Perfusion	9.96 min	0.7 mm	Diffusion/glutamine synthetase	80 %
^{82}Rb	Perfusion	76 s	2.6 mm	Na/K-ATPase	50–60 %
^{15}O-water	Perfusion	2.07 min	1.1 mm	Diffusion	Diffusible
^{18}F-FDG	Viability and inflammation	109.7 min	0.2 mm	Glucose transporter/hexokinase	1–3 %

PET positron emission tomography, *^{13}N-ammonia* nitrogen-13 ammonia, *^{82}Rb* rubidium-82, *^{15}O-water* oxygen-15 water, *^{18}F-FDG* fluorine-18 fluorodeoxyglucose

Perfusion Tracers Three PET perfusion tracers are currently available for clinical use, namely nitrogen-13 ammonia (^{13}N-ammonia), rubidium-82 (^{82}Rb), and oxygen-15 water (^{15}O-water).

Nitrogen-13 ammonia is generated in a cyclotron by bombarding ^{16}O-water with protons via the ^{16}O (p, α) ^{13}N reaction. In vivo, ^{13}N-ammonia is passively taken up into myocytes by diffusion, equilibrates intracellularly with its charged form ammonium (NH_4), and is finally trapped into the amino acid glutamine by the enzyme glutamine synthetase, resulting in ^{13}N-glutamine [20–23]. The first-pass trapping is high at rest, despite back diffusion, but decreases successively at higher coronary blood flow rates [24, 25]. Importantly, the overall trapping of ^{13}N-ammonia is dependant on an intact cardiac metabolism, which can be impaired during ischemia or high cardiac workload. ^{13}N-ammonia generates high-quality perfusion images with a high resolution and enables due to its short half-life a brief imaging protocol (Fig. 1).

Rubidium-82, produced in commercially available generators by the decay of strontium-82 (half-life 25.3 days, high energy cyclotron product) that is attached to an eluting column, is a monovalent cationic analog to potassium, which is taken up into myocytes by the Na/K-ATPase. The extraction fraction decreases in a non-linear manner with the increasing coronary blood flow [26–28], which is more pronounced compared with ^{13}N-ammonia, but still superior compared to technetium-99m-labeled SPECT tracers. Overall, the uptake of ^{82}Rb is a function of coronary blood flow, myocardial metabolism, and cell integrity, which can be altered by severe acidosis, hypoxia, and ischemia [29, 30]. Unfortunately, ^{82}Rb is not able to take full advantage of the superior image quality of PET due to the overall low count rates, a result of the short half-life of 76 s, and the emission of a high-energy positron, which leads to a poorer spatial resolution as it travels a longer distance before annihilation.

Oxygen-15 water is partially generated in a cyclotron by the ^{15}N (p, n) ^{15}O reaction resulting in ^{15}O-oxygen, which is subsequently transferred to a ^{15}O-water generator. In vivo, ^{15}O-water is metabolically inert, diffuses freely across membranes until it reaches equilibrium between compartments and has a very high linear myocardial extraction over a wide range of coronary blood flow rates. Importantly, cardiac uptake and release of ^{15}O-water is solely dependant on myocardial perfusion [12]. These properties make ^{15}O-water to an excellent quantification method for the MBF and CFR, but also results in a poor contrast between myocardium and blood pool, which requires complex subtraction algorithms of the blood pool activity prior to image reconstruction [12, 31, 32].

Myocardial perfusion imaging (MPI) is usually performed with the help of pharmacological stress, as for instance dipyridamole, adenosine, or regadenoson. Alternatively, exercise stress testing is in principle possible with ^{13}N-ammonia, and satisfactory results are even achievable with ^{82}Rb and ^{15}O-water [33–35], although very rarely performed in clinical practice.

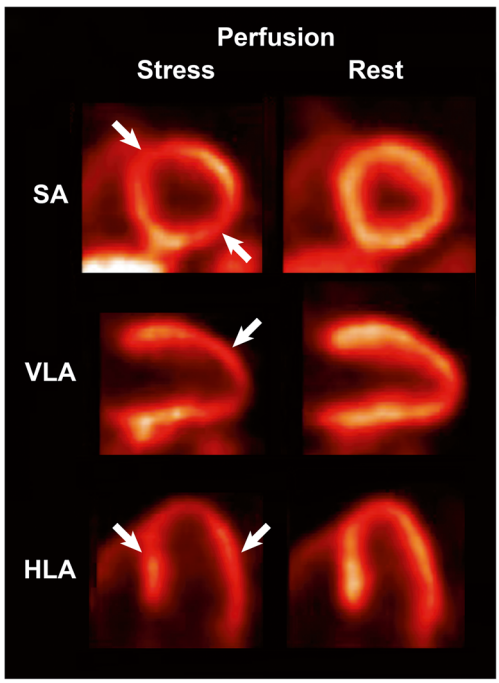

Fig. 1 PET perfusion imaging for the assessment of stable coronary artery disease. Large stress-induced myocardial perfusion defects, as indicated by *white arrows*, are shown in this patient who underwent a PET myocardial perfusion imaging study, using ^{13}N-ammonia as tracer, for the further diagnostic work-up of suspected coronary artery disease. *HLA* horizontal long-axis, *PET* positron emission tomography, *SA* short-axis, *VLA* vertical long-axis

Viability and Inflammation Tracer Fluorine-18 fluorodeoxyglucose (^{18}F-FDG), an analog of glucose, is the clinically available and well-established viability and inflammation tracer. The tracer is produced by labeling 2-deoxyglucose with fluorine-18, which is generated in a cyclotron by bombarding ^{18}O-enriched water with a proton beam. In vivo, ^{18}F-FDG is transported into cells by facilitated diffusion using specific glucose transporters (GLUT-1 and GLUT-4) and is subsequently phosphorylated by the enzyme hexokinase, which factually traps the tracer in the cell as the levels of the enzyme glucose-6-phosphatase, catalyzing the reverse reaction, are low [36]. FDG-6-phosphate is subsequently not metabolized any further. Additionally, it has been shown that the cellular uptake of ^{18}F-FDG can be used as a surrogate marker of the myocardial uptake and utilization of exogenous glucose [37].

The rational behind ^{18}F-FDG as a viability and inflammation tracer are the following observations: First, glucose uptake and metabolism are increased during states of hypoxia and mild-to-moderate ischemia, reduced in cases of severe ischemia, and absent in areas with scar tissue [38, 39]. Second, glucose uptake and metabolism are increased in inflammatory cells, through the overexpression of glucose transporters and glycolytic enzymes, which infiltrate tissue in different states of inflammatory disease [40–42].

In general, ^{18}F-FDG enables high-quality images, but only after thorough patient preparation to achieve homogenous glucose uptake for viability (using oral glucose loading, nicotinic acid derivatives, or an insulin and glucose infusion [43, 44]) and effective myocardial suppression for inflammation imaging (using prolonged fasting, high-fat and/or low-carbohydrate diet, or a heparin load [45–49]).

Issue of Radiation Exposure

In recent years, the number of cardiac imaging studies has increased considerably [50], which contributes to an overall substantial radiation exposure [51–53]. The potential for harm of low-dose ionizing radiation, as occurring during medical imaging, is still a matter of debate, but it is generally acknowledged that it might be harmful and that it should be kept at the lowest possible level, as doses can accumulate over a person's lifetime and result in a higher likelihood for developing malignancies ("linear no-threshold concept") [54]. This is of special importance in women and younger patients, especially children. Furthermore, this implies that PET should only be used when appropriate, optimized study protocols are applied to minimize radiation exposure, and other imaging modalities with comparable diagnostic accuracy have been considered but deemed inferior or not suitable [55]. From an individualized, patient-centered imaging perspective, the overall goal should be to reach a comprehensive diagnosis with as few investigations and the lowest radiation exposure as possible.

Established Clinical Applications

Myocardial Perfusion Imaging

Evaluation of Stable Coronary Artery Disease Myocardial perfusion imaging is performed in patients with suspected or known stable CAD with the aim to evaluate the presence and extent or absence of myocardial ischemia, as these findings should guide the further clinical decision-making process and overall choice of therapy. Importantly, non-invasive imaging should only be performed in patients with an intermediate pre-test probability for stable CAD, as it is clinically most useful and appropriate to use in this patient population [56, 57]. The assessment of the pre-test probability, which is mainly determined by the patients age, gender, and nature of symptoms, but also by the prevalence of CAD and presence of cardiovascular risk factors [58, 59], should be an integral part of the clinical decision-making process, as the interpretation of non-invasive imaging tests is based on the Bayesian approach to diagnosis. Hereby, it should be kept in mind that patients with an intermediate pre-test probability constitute clinically a quite heterogeneous group, which makes the choice of imaging strategy challenging and not solvable by using a one-test/one-protocol strategy for all patients.

Myocardial perfusion imaging using PET has, in comparison with other clinically available tests for the diagnosis of CAD, an extremely high diagnostic accuracy. Mc Ardle et al. [60] showed in a meta-analysis, which used invasive coronary angiography as reference, that ^{82}Rb PET has a superior diagnostic accuracy even compared with contemporary SPECT technology, with a sensitivity of 90 % (95 % confidence interval (CI) 0.88–0.92) and a specificity of 88 % (95 % CI 0.85–0.91). In a further recent meta-analysis, which compared MPI obtained by SPECT, CMR, and PET, using invasive coronary angiography as reference, PET achieved the highest diagnostic performance with a sensitivity of 84 % (95 % CI 0.81–0.87)/77 % (95 % CI 0.73–0.81) and specificity of 81 % (95 % CI 0.74–0.87)/88 % (95 % CI 0.84–0.90) on the patient and vessel level, respectively [61]. Finally, in a second recent meta-analysis, which compared MPI by SPECT, echocardiography, cardiac CT, CMR, and PET, using invasive coronary angiography with fractional flow reserve as reference, PET could successfully demonstrate hemodynamically significant CAD with a sensitivity of 84 % (95 % CI 0.75–0.91)/83 % (95 % CI 0.77–0.88), specificity of 87 % (95 % CI 0.80–0.92)/89 % (95 % CI 0.86–0.91), and negative likelihood ratio of 0.14 (95 % CI 0.02–0.87)/0.15 (95 % CI 0.05–0.44) on the patient and vessel level, respectively [62•]. CMR and cardiac CT showed a similar ability, in contrast to SPECT and echocardiography that were less suited for this purpose.

Flow Quantification Visual and semi-quantitative assessment of myocardial perfusion defects, as regularly performed

in SPECT and PET MPI, is based on the relative regional distribution of the perfusion tracer in the myocardium, using the region with the highest tracer uptake as "normal reference region," which is in case of a semi-quantitative analysis often further compared towards a database (Fig. 1). However, it has to be taken into account that the so-called "normal reference region" itself can be abnormal due to underlying multivessel disease, or the tracer uptake can be homogenously reduced in the entire LV myocardium, as in multivessel disease with "balanced ischemia." Under these circumstances, MPI can underestimate the true extent of ischemia or even miss the diagnosis of "balanced ischemia" [63–66]. In this context, it should be mentioned that a false-negative SPECT MPI is, despite all that, more frequently due to single-vessel disease than multivessel disease [67, 68]. Absolute quantification of regional MBF in milliliters per gram per minute, which can be routinely performed in clinical practice, overcomes these obstacles. In general, MBF is obtained during rest and under maximum stress, from which the CFR can be calculated as the ratio of the maximum (hyperemic) MBF to resting MBF. It has to be kept in mind that several factors, amongst others age, influence the obtained MBF during rest and stress and, thereby, the calculated CFR [69, 70]. In the presence of epicardial CAD, CFR can be used to assess the functional significance of a stenosis, as CFR decreases in proportion to the degree of the luminal narrowing [71, 72]. However, high individual flow variability can be observed in stenoses of intermediate severity. In contrast, in the absence of epicardial CAD, a reduced CFR reflects microvascular disease/dysfunction. Consequently, information concerning the status of the epicardial coronary arteries is necessary for a conclusive CFR interpretation, which can either be obtained by cardiac CT (for instance elegantly using hybrid imaging) or invasive coronary angiography.

Prognostic Value The greatest value of PET MPI, besides its high diagnostic accuracy, is its ability to predict adverse cardiac events. Dorbala et al. [73] demonstrated that patients with a normal ^{82}Rb MPI scan have a low annual cardiac mortality rate of 0.2 %, in contrast to a severely ischemic scan with a high annual cardiac mortality rate of 4.3 %. Furthermore, the results from a multicenter observational registry showed that the risk-adjusted hazard ratio of cardiac death increases successively for every 10 % raise in ischemic myocardium, namely from 2.3 (95 % CI 1.4–3.8) in mild to 4.9 (95 % CI 2.5–9.6) in severe ischemia [74]. Based on the current evidence, one can state that patients with a normal scan have a low annual cardiac event rate of <1 %, while an abnormal scan indicates worse prognosis with a continuous increase in risk in relation to the degree of ischemic burden [19, 73–75]. Furthermore, it has been shown that this outcome information is useful as a gatekeeper for invasive procedures as well as for the overall guidance of therapy based on the individual patient risk. Based on the extent of the determined perfusion deficit, PET MPI scans can be categorized into low (<5 % ischemic myocardium), intermediate (5–10 % ischemic myocardium), and high risk scans (>10 % ischemic myocardium). Further high-risk imaging features are as follows: transient LV cavity dilatation (sign for extensive LV dysfunction or ischemic burden) [76], increased tracer uptake in the lung (sign for severe LV dysfunction or ischemic burden), reduced LV rest/stress ejection fraction, and ejection fraction reserve (incremental prognostic value over perfusion deficit; sign for severe ischemia due to left main or three-vessel disease) [73, 77, 78], transient increased right ventricular tracer uptake (sign for severe ischemia due to left main or three-vessel disease) [79], and reduced CFR (incremental prognostic value over perfusion deficit; and marker of normal vascular reactivity) [80–83]. Observational evidence indicates that patients with <10 % ischemic myocardium experience a reduced risk of death receiving medical therapy alone as compared with coronary revascularization, while patients with ≥10 % ischemic myocardium encounter a reduced risk of death when undergoing coronary revascularization as compared with medical therapy [84–86, 87•]. Consequently, patients with a high risk PET MPI have, according to current guidelines, an indication for coronary revascularization [56, 57, 88••, 89].

Potential Clinical Applications The final choice of imaging modality and diagnostic algorithm is usually based on the respective local expertise, availability of the different imaging techniques, and overall economical resources. Table 2 summarizes potential clinical applications of PET MPI in the diagnosis of stable CAD, which are based on the techniques strengths and currently available evidence.

Myocardial Viability Imaging

Viability imaging is performed in patients with chronic ischemic cardiomyopathy, with the aim to identifying those patients, which might benefit from revascularization therapy, as the general procedure-related risk is high in this patient population.

Cardiac PET uses a combination of rest perfusion imaging and glucose metabolism imaging for the assessment of myocardial viability [90–93]. The subsequent comparison of the perfusion versus the metabolism images can identify one of four distinctive diagnostic patterns (Table 3). The first pattern, with both normal perfusion and glucose metabolism, is characteristic for *healthy myocardium* (Fig. 2). The second, the so-called "perfusion-metabolism mismatch" pattern, distinguished by a reduced perfusion but a preserved or enhanced glucose metabolism, indicates *viable myocardium* (Fig. 2). The presence of this mismatch pattern has been shown to be associated with an outcome benefit after revascularization [90, 94–96]. According to a meta-analysis by Inaba et al. [97], the

Table 2 Potential clinical applications of cardiac PET

Myocardial perfusion imaging (quantitative analysis)
- Evaluation of functional significance of known coronary artery stenosis (as for instance diagnosed by prior CTA)
- Evaluation of complex stable coronary artery disease with or without suspected "balanced ischemia"
- Evaluation of suspected microvascular disease/dysfunction
- Challenging body habitus (obese patients, women with large breasts)
- Contraindications for other imaging modalities (as for instance due to metallic implants)
- Second-line test after other non-diagnostic imaging study

Myocardial viability imaging
- Advanced ischemic cardiomyopathy with severe left ventricular dysfunction (EF <35 %)
- Second-line test in cases where therapeutic decision is still uncertain after first imaging study

Inflammation imaging
- Evaluation of disease activity and response to treatment in cardiac sarcoidosis
- Evaluation of difficult cases of prosthetic valve endocarditis and cardiac device infections

CTA computed tomography angiography, *EF* ejection fraction; otherwise, abbreviations as in Table 1

optimal amount of viable myocardium required for a survival benefit from revascularization was estimated to be 25.8 % (95 % CI 16.6–35 %). The third, the so-called "perfusion-metabolism match" pattern, with both reduced perfusion as well as glucose metabolism, signifies *non-viable myocardium/scar* (Fig. 2), which is a further independent predictor of LV function recovery after revascularization [91]. The fourth, the so-called "perfusion-metabolism reverse mismatch" pattern is characterized by a preserved perfusion but a reduced glucose metabolism (Fig. 2). The clinical significance of this regionally altered glucose metabolism is unknown, but it has been observed in patients with non-ischemic cardiomyopathy, left bundle branch block, repetitive stunning, diabetes mellitus, as well as early after revascularization in myocardial infarction. Furthermore, it has been suggested that reverse mismatch in the septum might be a predictor of response to cardiac resynchronization therapy [98].

Several imaging techniques are available for the assessment of myocardial viability, all looking at different pathophysiological aspects, which explains the occurrence of incongruent results. PET, based on the assessment of cellular integrity/metabolism, has in comparison with all other imaging modalities the highest sensitivity in predicting regional function recovery after revascularization, in contrast to dobutamine stress echocardiography, which has the highest specificity by assessing the contractile reserve [99]. PET viability imaging is, according to current evidence and expert-opinion, preferred over SPECT, especially in patients with severe LV dysfunction [9, 100].

Predictive and Prognostic Value PET viability imaging can accurately predict improvement of regional wall motion, global LV ejection fraction, heart failure symptoms, and exercise capacity following revascularization. The highest predictive value can be obtained when perfusion is reduced >50 % and glucose uptake is simultaneously relative high. According to a meta-analysis by Schinkel et al. [99], PET can predict the regional function recovery with a weighted mean sensitivity of 92 % and a specificity of 63 %, as well as the global contractile function recovery with a weighted mean sensitivity of 83 % and a specificity of 64 %. Furthermore, it has been shown that patients with PET-defined viable myocardium should undergo revascularization as soon as possible, as every delay in intervention will make an improvement less likely [101, 102]. Additionally, PET can provide prognostic information in patients with ischemic cardiomyopathy in relation to their PET findings and their chosen treatment strategy. In patients with viable myocardium, a meta-analysis determined an annualized mortality rate of 4 % when undergoing revascularization versus 17 % when receiving medical treatment, and in patients with non-viable myocardium, the reported annualized mortality rate was 6 % when undergoing revascularization versus 8 % when receiving medical treatment [99]. Finally, assessment of myocardial viability by PET has been explored in the randomized PARR-2 trial, which investigated the effectiveness of PET-assisted management in patients with severe LV dysfunction and suspected CAD. The study demonstrated overall no significant reduction in cardiac events for PET-assisted management versus standard

Table 3 Simplified rest perfusion-metabolism (^{18}F-FDG) patterns in PET viability imaging

Myocardial state	Perfusion	Metabolism
Healthy	Normal	Normal
Viable	Reduced	Preserved/enhanced
"Perfusion-metabolism mismatch"		
Non-viable/scar	Reduced	Reduced
"Perfusion-metabolism match"		
Altered regional glucose metabolism	Preserved	Reduced
"Perfusion-metabolism reverse mismatch"		

Abbreviations as in Tables 1 and 2

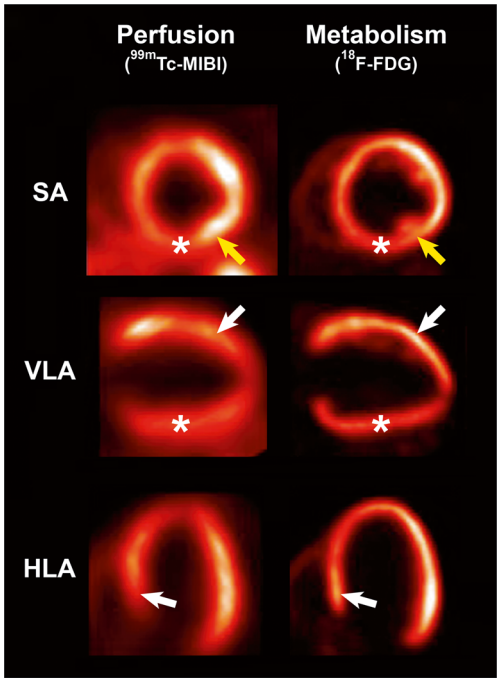

Fig. 2 PET perfusion-metabolism imaging for the assessment of myocardial viability. This study of a patient with chronic ischemic cardiomyopathy, which utilized a combination of single-photon emission computed tomography for myocardial rest perfusion imaging and PET for metabolism imaging, illustrates typical rest perfusion-metabolism patterns as encountered in viability imaging. *Healthy myocardium* can be found in the lateral wall segments. *Viable myocardium*, as indicated by a "perfusion-metabolism mismatch," is for instance present in the septal and anterior wall segments, as indicated by *white arrows*. *Non-viable myocardium*, as indicated by a "perfusion-metabolism match," can for instance be found in the inferior wall, as indicated by *white stars*. Finally, an *altered regional glucose metabolism*, as indicated by a "perfusion-metabolism reverse mismatch," can be suspected in the inferolateral wall (*yellow arrows*). *^{18}F-FDG* fluorine-18 fluorodeoxyglucose, *^{99m}Tc-MIBI* technetium sestamibi; otherwise, abbreviations as in Fig. 1

care. Hereby should be kept in mind that non-adherence to PET-based recommendations was found in 25 % of the included patients. However, in a post hoc subgroup analysis (ADHERE arm) adherence to PET-based recommendations regarding therapy resulted in a significant survival benefit [92]. In a further post hoc subgroup analysis, PET-guided management resulted, in the setting of an experienced imaging center, also in a significant reduction in cardiac events [103]. Taken together, PET viability imaging has the clinical ability to identify high-risk patients with severe LV dysfunction (ejection fraction <35 %) who may benefit from revascularization, although further evidence is needed.

Potential Clinical Applications The final choice of imaging modality and diagnostic algorithm is, similar to those for the diagnosis of stable CAD, based on several local conditions. Table 2 summarizes potential clinical applications of PET viability imaging, which are based on the techniques strengths and currently available evidence.

Evolving Clinical Applications

Inflammation Imaging

Cardiac PET is a rapidly evolving imaging technique with many promising applications, like myocardial innervation imaging [104, 105], aiming at the identification of patients at high risk for sudden cardiac death or ventricular arrhythmia, or vulnerable plaque imaging [106, 107], which more or less all still search for their practical clinical role. In contrast, imaging of inflammatory cardiovascular disease has come a step further and stands for certain indications, as highlighted below, on the verge of routine clinical implementation, as more and more evidence of its usefulness accumulates. An in-depth review of this topic is beyond the scope of this article and the interested reader is referred to dedicated literature [108–110, 111•, 112, 113•].

Cardiac Sarcoidosis ^{18}F-FDG PET is, according to continuously growing evidence, a valuable tool in the difficult diagnosis of cardiac sarcoidosis, as it is currently the only imaging modality that can evaluate disease activity, monitor treatment response, and evaluate the overall degree of dissemination in the body (Table 2) [46, 114]. Although cardiac PET is not included as diagnostic criteria for cardiac sarcoidosis by the Japanese Ministry of Health and Welfare, it is considered part of the current state of the art work-up according to expert consensus [115, 116••]. This is partly due to promising results from a meta-analysis concerning the diagnostic accuracy of ^{18}F-FDG PET, which determined a pooled sensitivity of 89 % (95 % CI 0.79–0.96) and specificity of 78 % (95 % CI 0.68–0.86) [117]. Usually, ^{18}F-FDG PET studies describe the characteristic uptake pattern as focal (Fig. 3), diffuse or focal on diffuse, but the combination with rest MPI allows an even more detailed classification, namely in stages as early (inflammation without scar), progressive (combined inflammation and scar), and fibrotic (scar without inflammation) [114, 118]. Furthermore, it has been shown that the combination of a focal perfusion deficit and ^{18}F-FDG uptake identifies patients at higher risk for death or ventricular tachycardia [119•]. In the future, the method might reach its full potential in combination with CMR, which already has an established role in the diagnosis of cardiac sarcoidosis, by using a PET/CMR approach.

Infective Endocarditis and Cardiac Device Infections ^{18}F-FDG PET has shown promising results in patients with prosthetic valve endocarditis and cardiac device infections [110, 120–124]. Adding an abnormal ^{18}F-FDG uptake around a

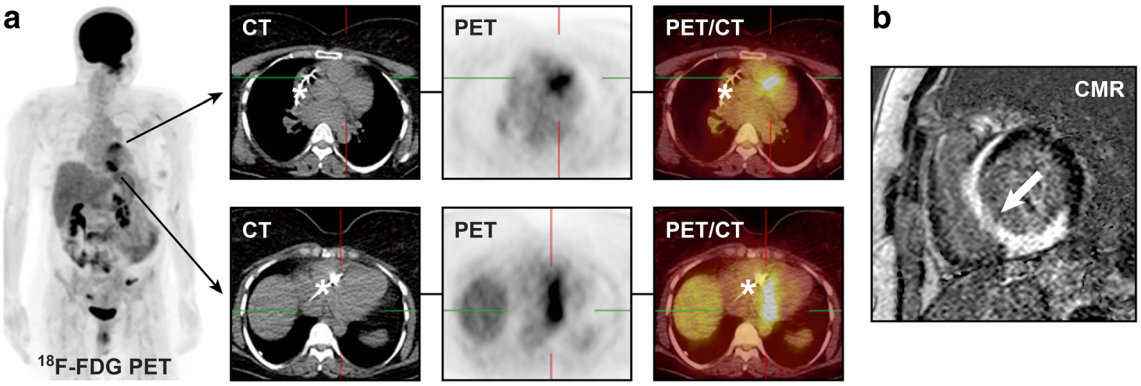

Fig. 3 ^{18}F-FDG PET for the assessment of cardiac sarcoidosis. In this patient with known sarcoidosis of the lungs, new-onset syncope and intermittent third-degree atrioventricular block, a cardiac PET study revealed an increased focal ^{18}F-FDG uptake in the septal and inferior wall segments, which is a finding consistent with an active cardiac engagement (**a**). Furthermore, extensive delayed enhancement (*white arrow*) was demonstrated in the same wall segments in a prior cardiovascular magnetic resonance (CMR) study (**b**). Permanent pacemaker electrode indicated by *white star*. *CT* computed tomography; otherwise, abbreviations as in Figs. 1 and 2

prosthetic valve as a new major criterion at admission increased, according to Saby et al. [125], the sensitivity of the modified Duke criteria from 70 % (95 % CI 0.52–0.83) to 97 % (95 % CI 0.83–0.99) for the diagnosis of prosthetic valve endocarditis (Fig. 4). Furthermore, the reported diagnostic accuracy in cardiac device infections is promising, with a sensitivity of 89 % (95 % CI 0.72–0.96) and a specificity of 86 % (95 % CI 0.42–0.99) [123]. In contrast, in native valve endocarditis, PET may only have limited usefulness, apart from the visualization of potential complications such as abscess formation, perivascular extension, or embolic infection events. Taken together, further evidence is needed before general recommendations can be made, but it seems that ^{18}F-FDG PET may be useful in difficult cases of infectious endocarditis and cardiac device infections (Table 2).

Cost-Effectiveness Considerations

Cost-effectiveness plays in every health system a more and more important role, due to overall limited resources in continuously aging populations. This is of special importance in the field of cardiac imaging with its extensive but also redundant possibilities. A comprehensive analysis of cost-effectiveness is a rather complex issue, as not only the cost of a single test, but also the indirect and induced costs of a management algorithm have to be taken into account. By this means, the high diagnostic accuracy of cardiac PET comes into play, as it can contribute to a reduction in additional costs caused by either unnecessary subsequent diagnostic/therapeutic procedures due to false positive tests or eventual complications due to false negative tests, despite its high costs of a single test. This aspect has been shown in a mathematical model by Patterson et al. [126], who compared the cost-effectiveness of exercise ECG, SPECT, PET, and invasive coronary angiography in the diagnosis of CAD. According to their model, PET showed the lowest cost per effect or cost per utility unit in patients with a pre-test probability <70 % for CAD. Similar results have also been found by Gould et al. [127]. These theoretical assumptions were confirmed in a prospective clinical study by Merhige et al. [128], which demonstrated that a PET-based algorithm in patients with intermediate pre-test probability for CAD could reduce the downstream use of invasive coronary angiography and thereby enable cost savings. Additionally, further aspects can contribute to cost savings, namely a high patient throughput in combination with the relatively short duration of PET imaging protocols, which also improves the overall patient comfort. Similar aspects have to be considered concerning the cost-effectiveness of PET viability imaging, which has a proven influence on clinical decision-making [129]. Furthermore, it has been shown that a PET-based selection of patients with poor LV function for coronary artery bypass grafting might be cost-

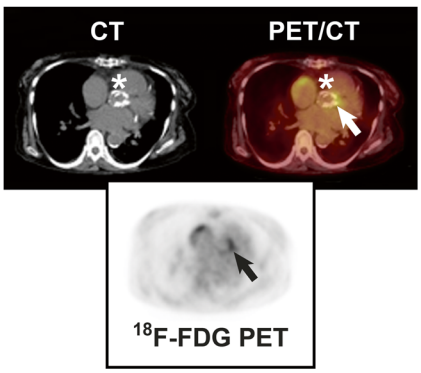

Fig. 4 ^{18}F-FDG PET for the assessment of prosthetic valve endocarditis. Abnormal ^{18}F-FDG uptake (*arrow*) is shown around a prosthetic aortic valve (*white star*), which suggests the presence of prosthetic valve endocarditis. Abbreviations as in Figs. 1, 2, and 3

effective [130]. Altogether, additional studies are needed to shed further light on this important but rather complex issue.

Conclusions

Cardiac PET is a valuable, quantitative, non-invasive imaging modality, which can be useful in the setting of an individualized, patient-centered imaging approach. Myocardial perfusion and viability imaging are, as a result of growing evidence for their diagnostic and prognostic usefulness, established clinical indications that may be cost-effective, due to the high diagnostic accuracy of cardiac PET, despite high single-test costs. Even new, promising clinical indications, as in the field of inflammation imaging, are entering the clinical arena and may contribute to a better diagnosis and overall patient care.

Acknowledgments The authors would like to thank Dr. Erika Fagman, Department of Radiology, Sahlgrenska University Hospital, Gothenburg/ Sweden, for providing valuable images for this article.

Compliance with Ethical Standards

Conflict of Interest Christian L. Polte, Iris Burck, Milan Lomsky, Peter Gjertsson, and Stephan G. Nekolla declare that they have no conflicts of interest. Eike Nagel reports research support from Siemens Healthcare, Bayer Healthcare, and Philips Healthcare; non-financial support from TomTec, CVI42, and MEDIS, during the conduct of the study; and personal fees from Bayer Healthcare, outside the submitted work.

Human and Animal Rights and Informed Consent This article does not contain any studies with human or animal subjects performed by any of the authors.

References

Papers of particular interest, published recently, have been highlighted as:
•& emsp;Of impor
ance •• Of major importance

1. Vogel R, Indermuhle A, Reinhardt J, Meier P, Siegrist PT, Namdar M, et al. The quantification of absolute myocardial perfusion in humans by contrast echocardiography: algorithm and validation. J Am Coll Cardiol. 2005;45:754–62.
2. Baer FM, Voth E, Deutsch HJ, Schneider CA, Schicha H, Sechtem U. Assessment of viable myocardium by dobutamine transesophageal echocardiography and comparison with fluorine-18 fluorodeoxyglucose positron emission tomography. J Am Coll Cardiol. 1994;24:343–53.
3. Bonow RO, Dilsizian V, Cuocolo A, Bacharach SL. Identification of viable myocardium in patients with chronic coronary artery disease and left ventricular dysfunction. Comparison of thallium scintigraphy with reinjection and PET imaging with 18F-fluorodeoxyglucose. Circulation. 1991;83:26–37.
4. Dilsizian V, Arrighi JA, Diodati JG, Quyyumi AA, Alavi K, Bacharach SL, et al. Myocardial viability in patients with chronic coronary artery disease. Comparison of 99mTc-sestamibi with thallium reinjection and [18F]fluorodeoxyglucose. Circulation. 1994;89:578–87.
5. Schwitter J, Nanz D, Kneifel S, Bertschinger K, Buchi M, Knusel PR, et al. Assessment of myocardial perfusion in coronary artery disease by magnetic resonance: a comparison with positron emission tomography and coronary angiography. Circulation. 2001;103:2230–5.
6. Baer FM, Voth E, Schneider CA, Theissen P, Schicha H, Sechtem U. Comparison of low-dose dobutamine-gradient-echo magnetic resonance imaging and positron emission tomography with [18F]fluorodeoxyglucose in patients with chronic coronary artery disease. A functional and morphological approach to the detection of residual myocardial viability. Circulation. 1995;91:1006–15.
7. Klein C, Nekolla SG, Bengel FM, Momose M, Sammer A, Haas F, et al. Assessment of myocardial viability with contrast-enhanced magnetic resonance imaging: comparison with positron emission tomography. Circulation. 2002;105:162–7.
8. Knuesel PR, Nanz D, Wyss C, Buechi M, Kaufmann PA, von Schulthess GK, et al. Characterization of dysfunctional myocardium by positron emission tomography and magnetic resonance: relation to functional outcome after revascularization. Circulation. 2003;108:1095–100.
9. Le Guludec D, Lautamaki R, Knuuti J, Bax JJ, Bengel FM. Present and future of clinical cardiovascular PET imaging in Europe—a position statement by the European Council of Nuclear Cardiology (ECNC). Eur J Nucl Med Mol Imaging. 2008;35:1709–24.
10. Muzik O, Beanlands RS, Hutchins GD, Mangner TJ, Nguyen N, Schwaiger M. Validation of nitrogen-13-ammonia tracer kinetic model for quantification of myocardial blood flow using PET. J Nucl Med. 1993;34:83–91.
11. Lautamaki R, George RT, Kitagawa K, Higuchi T, Merrill J, Voicu C, et al. Rubidium-82 PET-CT for quantitative assessment of myocardial blood flow: validation in a canine model of coronary artery stenosis. Eur J Nucl Med Mol Imaging. 2009;36:576–86.
12. Bergmann SR, Fox KA, Rand AL, McElvany KD, Welch MJ, Markham J, et al. Quantification of regional myocardial blood flow in vivo with H215O. Circulation. 1984;70:724–33.
13. Slomka PJ, Dey D, Duvall WL, Henzlova MJ, Berman DS, Germano G. Advances in nuclear cardiac instrumentation with a view towards reduced radiation exposure. Curr Cardiol Rep. 2012;14:208–16.
14. Slomka PJ, Berman DS, Germano G. New cardiac cameras: single-photon emission CT and PET. Semin Nucl Med. 2014;44:232–51.
15. Slomka PJ, Pan T, Berman DS, Germano G. Advances in SPECT and PET hardware. Prog Cardiovasc Dis. 2015;57:566–78.
16. Koepfli P, Hany TF, Wyss CA, Namdar M, Burger C, Konstantinidis AV, et al. CT attenuation correction for myocardial perfusion quantification using a PET/CT hybrid scanner. J Nucl Med. 2004;45:537–42.
17. Souvatzoglou M, Bengel F, Busch R, Kruschke C, Fernolendt H, Lee D, et al. Attenuation correction in cardiac PET/CT with three different CT protocols: a comparison with conventional PET. Eur J Nucl Med Mol Imaging. 2007;34:1991–2000.
18. Bateman TM, Heller GV, McGhie AI, Friedman JD, Case JA, Bryngelson JR, et al. Diagnostic accuracy of rest/stress ECG-gated Rb-82 myocardial perfusion PET: comparison with ECG-gated Tc-99m sestamibi SPECT. J Nucl Cardiol. 2006;13:24–33.
19. Yoshinaga K, Chow BJ, Williams K, Chen L, deKemp RA, Garrard L, et al. What is the prognostic value of myocardial perfusion imaging using rubidium-82 positron emission tomography? J Am Coll Cardiol. 2006;48:1029–39.
20. Schelbert HR, Phelps ME, Hoffman EJ, Huang SC, Selin CE, Kuhl DE. Regional myocardial perfusion assessed with N-13

labeled ammonia and positron emission computerized axial tomography. Am J Cardiol. 1979;43:209–18.
21. Schelbert HR, Phelps ME, Huang SC, MacDonald NS, Hansen H, Selin C, et al. N-13 ammonia as an indicator of myocardial blood flow. Circulation. 1981;63:1259–72.
22. Bergmann SR, Hack S, Tewson T, Welch MJ, Sobel BE. The dependence of accumulation of 13NH3 by myocardium on metabolic factors and its implications for quantitative assessment of perfusion. Circulation. 1980;61:34–43.
23. Krivokapich J, Huang SC, Phelps ME, MacDonald NS, Shine KI. Dependence of 13NH3 myocardial extraction and clearance on flow and metabolism. Am J Physiol. 1982;242:H536–42.
24. Nienaber CA, Ratib O, Gambhir SS, Krivokapich J, Huang SC, Phelps ME, et al. A quantitative index of regional blood flow in canine myocardium derived noninvasively with N-13 ammonia and dynamic positron emission tomography. J Am Coll Cardiol. 1991;17:260–9.
25. Yoshida K, Mullani N, Gould KL. Coronary flow and flow reserve by PET simplified for clinical applications using rubidium-82 or nitrogen-13-ammonia. J Nucl Med. 1996;37:1701–12.
26. Mack RE, Nolting DD, Hogancamp CE, Bing RJ. Myocardial extraction of Rb-86 in the rabbit. Am J Physiol. 1959;197:1175–7.
27. Becker L, Ferreira R, Thomas M. Comparison of 86Rb and microsphere estimates of left ventricular bloodflow distribution. J Nucl Med. 1974;15:969–73.
28. Lortie M, Beanlands RS, Yoshinaga K, Klein R, Dasilva JN, DeKemp RA. Quantification of myocardial blood flow with 82Rb dynamic PET imaging. Eur J Nucl Med Mol Imaging. 2007;34:1765–74.
29. Goldstein RA, Mullani NA, Marani SK, Fisher DJ, Gould KL, O'Brien Jr HA. Myocardial perfusion with rubidium-82. II. Effects of metabolic and pharmacologic interventions. J Nucl Med. 1983;24:907–15.
30. Selwyn AP, Allan RM, L'Abbate A, Horlock P, Camici P, Clark J, et al. Relation between regional myocardial uptake of rubidium-82 and perfusion: absolute reduction of cation uptake in ischemia. Am J Cardiol. 1982;50:112–21.
31. Bol A, Melin JA, Vanoverschelde JL, Baudhuin T, Vogelaers D, De Pauw M, et al. Direct comparison of [13N]ammonia and [15O]water estimates of perfusion with quantification of regional myocardial blood flow by microspheres. Circulation. 1993;87:512–25.
32. Kajander SA, Joutsiniemi E, Saraste M, Pietila M, Ukkonen H, Saraste A, et al. Clinical value of absolute quantification of myocardial perfusion with (15)O-water in coronary artery disease. Circ Cardiovasc Imaging. 2011;4:678–84.
33. Chow BJ, Beanlands RS, Lee A, DaSilva JN, deKemp RA, Alkahtani A, et al. Treadmill exercise produces larger perfusion defects than dipyridamole stress N-13 ammonia positron emission tomography. J Am Coll Cardiol. 2006;47:411–6.
34. Chow BJ, Ananthasubramaniam K, dekemp RA, Dalipaj MM, Beanlands RS, Ruddy TD. Comparison of treadmill exercise versus dipyridamole stress with myocardial perfusion imaging using rubidium-82 positron emission tomography. J Am Coll Cardiol. 2005;45:1227–34.
35. Wyss CA, Koepfli P, Mikolajczyk K, Burger C, von Schulthess GK, Kaufmann PA. Bicycle exercise stress in PET for assessment of coronary flow reserve: repeatability and comparison with adenosine stress. J Nucl Med. 2003;44:146–54.
36. Gallagher BM, Ansari A, Atkins H, Casella V, Christman DR, Fowler JS, et al. Radiopharmaceuticals XXVII. 18F-labeled 2-deoxy-2-fluoro-d-glucose as a radiopharmaceutical for measuring regional myocardial glucose metabolism in vivo: tissue distribution and imaging studies in animals. J Nucl Med. 1977;18:990–6.
37. Ratib O, Phelps ME, Huang SC, Henze E, Selin CE, Schelbert HR. Positron tomography with deoxyglucose for estimating local myocardial glucose metabolism. J Nucl Med. 1982;23:577–86.
38. Bing RJ. Cardiac metabolism. Physiol Rev. 1965;45:171–213.
39. Camici P, Ferrannini E, Opie LH. Myocardial metabolism in ischemic heart disease: basic principles and application to imaging by positron emission tomography. Prog Cardiovasc Dis. 1989;32:217–38.
40. Mochizuki T, Tsukamoto E, Kuge Y, Kanegae K, Zhao S, Hikosaka K, et al. FDG uptake and glucose transporter subtype expressions in experimental tumor and inflammation models. J Nucl Med. 2001;42:1551–5.
41. Kubota R, Yamada S, Kubota K, Ishiwata K, Tamahashi N, Ido T. Intratumoral distribution of fluorine-18-fluorodeoxyglucose in vivo: high accumulation in macrophages and granulation tissues studied by microautoradiography. J Nucl Med. 1992;33:1972–80.
42. Gamelli RL, Liu H, He LK, Hofmann CA. Augmentations of glucose uptake and glucose transporter-1 in macrophages following thermal injury and sepsis in mice. J Leukoc Biol. 1996;59:639–47.
43. Knuuti MJ, Nuutila P, Ruotsalainen U, Saraste M, Harkonen R, Ahonen A, et al. Euglycemic hyperinsulinemic clamp and oral glucose load in stimulating myocardial glucose utilization during positron emission tomography. J Nucl Med. 1992;33:1255–62.
44. Knuuti MJ, Yki-Jarvinen H, Voipio-Pulkki LM, Maki M, Ruotsalainen U, Harkonen R, et al. Enhancement of myocardial [fluorine-18]fluorodeoxyglucose uptake by a nicotinic acid derivative. J Nucl Med. 1994;35:989–98.
45. Ishimaru S, Tsujino I, Takei T, Tsukamoto E, Sakaue S, Kamigaki M, et al. Focal uptake on 18F-fluoro-2-deoxyglucose positron emission tomography images indicates cardiac involvement of sarcoidosis. Eur Heart J. 2005;26:1538–43.
46. Ambrosini V, Zompatori M, Fasano L, Nanni C, Nava S, Rubello D, et al. (18)F-FDG PET/CT for the assessment of disease extension and activity in patients with sarcoidosis: results of a preliminary prospective study. Clin Nucl Med. 2013;38:e171–7.
47. Williams G, Kolodny GM. Suppression of myocardial 18F-FDG uptake by preparing patients with a high-fat, low-carbohydrate diet. AJR Am J Roentgenol. 2008;190:W151–6.
48. Cheng VY, Slomka PJ, Ahlen M, Thomson LE, Waxman AD, Berman DS. Impact of carbohydrate restriction with and without fatty acid loading on myocardial 18F-FDG uptake during PET: a randomized controlled trial. J Nucl Cardiol. 2010;17:286–91.
49. Harisankar CN, Mittal BR, Agrawal KL, Abrar ML, Bhattacharya A. Utility of high fat and low carbohydrate diet in suppressing myocardial FDG uptake. J Nucl Cardiol. 2011;18:926–36.
50. Smith-Bindman R, Miglioretti DL, Johnson E, Lee C, Feigelson HS, Flynn M, et al. Use of diagnostic imaging studies and associated radiation exposure for patients enrolled in large integrated health care systems, 1996–2010. JAMA. 2012;307:2400–9.
51. Fazel R, Krumholz HM, Wang Y, Ross JS, Chen J, Ting HH, et al. Exposure to low-dose ionizing radiation from medical imaging procedures. N Engl J Med. 2009;361:849–57.
52. Chen J, Einstein AJ, Fazel R, Krumholz HM, Wang Y, Ross JS, et al. Cumulative exposure to ionizing radiation from diagnostic and therapeutic cardiac imaging procedures: a population-based analysis. J Am Coll Cardiol. 2010;56:702–11.
53. Einstein AJ, Moser KW, Thompson RC, Cerqueira MD, Henzlova MJ. Radiation dose to patients from cardiac diagnostic imaging. Circulation. 2007;116:1290–305.
54. Hendee WR, O'Connor MK. Radiation risks of medical imaging: separating fact from fantasy. Radiology. 2012;264:312–21.
55. Cerqueira MD, Allman KC, Ficaro EP, Hansen CL, Nichols KJ, Thompson RC, et al. Recommendations for reducing radiation exposure in myocardial perfusion imaging. J Nucl Cardiol. 2010;17:709–18.

56. Montalescot G, Sechtem U, Achenbach S, Andreotti F, Arden C, Budaj A, et al. 2013 ESC guidelines on the management of stable coronary artery disease: the task force on the management of stable coronary artery disease of the European Society of Cardiology. Eur Heart J. 2013;34:2949–3003.
57. Fihn SD, Gardin JM, Abrams J, Berra K, Blankenship JC, Dallas AP, et al. 2012 ACCF/AHA/ACP/AATS/PCNA/SCAI/STS guideline for the diagnosis and management of patients with stable ischemic heart disease: executive summary: a report of the American College of Cardiology Foundation/American Heart Association task force on practice guidelines, and the American College of Physicians, American Association for Thoracic Surgery, Preventive Cardiovascular Nurses Association, Society for Cardiovascular Angiography and Interventions, and Society of Thoracic Surgeons. Circulation. 2012;126:3097–137.
58. Diamond GA, Forrester JS. Analysis of probability as an aid in the clinical diagnosis of coronary-artery disease. N Engl J Med. 1979;300:1350–8.
59. Genders TS, Steyerberg EW, Alkadhi H, Leschka S, Desbiolles L, Nieman K, et al. A clinical prediction rule for the diagnosis of coronary artery disease: validation, updating, and extension. Eur Heart J. 2011;32:1316–30.
60. Mc Ardle BA, Dowsley TF, deKemp RA, Wells GA, Beanlands RS. Does rubidium-82 PET have superior accuracy to SPECT perfusion imaging for the diagnosis of obstructive coronary disease?: a systematic review and meta-analysis. J Am Coll Cardiol. 2012;60:1828–37.
61. Jaarsma C, Leiner T, Bekkers SC, Crijns HJ, Wildberger JE, Nagel E, et al. Diagnostic performance of noninvasive myocardial perfusion imaging using single-photon emission computed tomography, cardiac magnetic resonance, and positron emission tomography imaging for the detection of obstructive coronary artery disease: a meta-analysis. J Am Coll Cardiol. 2012;59:1719–28.
62.• Takx RA, Blomberg BA, El Aidi H, Habets J, de Jong PA, Nagel E, et al. Diagnostic accuracy of stress myocardial perfusion imaging compared to invasive coronary angiography with fractional flow reserve meta-analysis. Circ Cardiovasc Imaging. 2015;8:e002666. **Meta-analysis of the diagnostic accuracy of stress myocardial perfusion imaging by single-photon emission computed tomography, echocardiography, magnetic resonance imaging, positron emission tomography and computed tomography using invasive coronary angiography with fractional flow reserve as reference**.
63. Lima RS, Watson DD, Goode AR, Siadaty MS, Ragosta M, Beller GA, et al. Incremental value of combined perfusion and function over perfusion alone by gated SPECT myocardial perfusion imaging for detection of severe three-vessel coronary artery disease. J Am Coll Cardiol. 2003;42:64–70.
64. Berman DS, Kang X, Slomka PJ, Gerlach J, de Yang L, Hayes SW, et al. Underestimation of extent of ischemia by gated SPECT myocardial perfusion imaging in patients with left main coronary artery disease. J Nucl Cardiol. 2007;14:521–8.
65. Beller GA. Underestimation of coronary artery disease with SPECT perfusion imaging. J Nucl Cardiol. 2008;15:151–3.
66. Ragosta M, Bishop AH, Lipson LC, Watson DD, Gimple LW, Sarembock IJ, et al. Comparison between angiography and fractional flow reserve versus single-photon emission computed tomographic myocardial perfusion imaging for determining lesion significance in patients with multivessel coronary disease. Am J Cardiol. 2007;99:896–902.
67. Yokota S, Ottervanger JP, Mouden M, Timmer JR, Knollema S, Jager PL. Prevalence, location, and extent of significant coronary artery disease in patients with normal myocardial perfusion imaging. J Nucl Cardiol. 2014;21:284–90.
68. Nishimura S, Mahmarian JJ, Boyce TM, Verani MS. Quantitative thallium-201 single-photon emission computed tomography during maximal pharmacologic coronary vasodilation with adenosine for assessing coronary artery disease. J Am Coll Cardiol. 1991;18:736–45.
69. Chareonthaitawee P, Kaufmann PA, Rimoldi O, Camici PG. Heterogeneity of resting and hyperemic myocardial blood flow in healthy humans. Cardiovasc Res. 2001;50:151–61.
70. Camici PG, Rimoldi OE. The clinical value of myocardial blood flow measurement. J Nucl Med. 2009;50:1076–87.
71. Uren NG, Melin JA, De Bruyne B, Wijns W, Baudhuin T, Camici PG. Relation between myocardial blood flow and the severity of coronary-artery stenosis. N Engl J Med. 1994;330:1782–8.
72. Di Carli M, Czernin J, Hoh CK, Gerbaudo VH, Brunken RC, Huang SC, et al. Relation among stenosis severity, myocardial blood flow, and flow reserve in patients with coronary artery disease. Circulation. 1995;91:1944–51.
73. Dorbala S, Hachamovitch R, Curillova Z, Thomas D, Vangala D, Kwong RY, et al. Incremental prognostic value of gated Rb-82 positron emission tomography myocardial perfusion imaging over clinical variables and rest LVEF. JACC Cardiovasc Imaging. 2009;2:846–54.
74. Dorbala S, Di Carli MF, Beanlands RS, Merhige ME, Williams BA, Veledar E, et al. Prognostic value of stress myocardial perfusion positron emission tomography: results from a multicenter observational registry. J Am Coll Cardiol. 2013;61:176–84.
75. Marwick TH, Shan K, Patel S, Go RT, Lauer MS. Incremental value of rubidium-82 positron emission tomography for prognostic assessment of known or suspected coronary artery disease. Am J Cardiol. 1997;80:865–70.
76. Rischpler C, Higuchi T, Fukushima K, Javadi MS, Merrill J, Nekolla SG, et al. Transient ischemic dilation ratio in 82Rb PET myocardial perfusion imaging: normal values and significance as a diagnostic and prognostic marker. J Nucl Med. 2012;53:723–30.
77. Dorbala S, Vangala D, Sampson U, Limaye A, Kwong R, Di Carli MF. Value of vasodilator left ventricular ejection fraction reserve in evaluating the magnitude of myocardium at risk and the extent of angiographic coronary artery disease: a 82Rb PET/CT study. J Nucl Med. 2007;48:349–58.
78. Lertsburapa K, Ahlberg AW, Bateman TM, Katten D, Volker L, Cullom SJ, et al. Independent and incremental prognostic value of left ventricular ejection fraction determined by stress gated rubidium 82 PET imaging in patients with known or suspected coronary artery disease. J Nucl Cardiol. 2008;15:745–53.
79. Abraham A, Kass M, Ruddy TD, deKemp RA, Lee AK, Ling MC, et al. Right and left ventricular uptake with Rb-82 PET myocardial perfusion imaging: markers of left main or 3 vessel disease. J Nucl Cardiol. 2010;17:52–60.
80. Murthy VL, Naya M, Foster CR, Hainer J, Gaber M, Di Carli G, et al. Improved cardiac risk assessment with noninvasive measures of coronary flow reserve. Circulation. 2011;124:2215–24.
81. Murthy VL, Naya M, Foster CR, Gaber M, Hainer J, Klein J, et al. Association between coronary vascular dysfunction and cardiac mortality in patients with and without diabetes mellitus. Circulation. 2012;126:1858–68.
82. Ziadi MC, Dekemp RA, Williams KA, Guo A, Chow BJ, Renaud JM, et al. Impaired myocardial flow reserve on rubidium-82 positron emission tomography imaging predicts adverse outcomes in patients assessed for myocardial ischemia. J Am Coll Cardiol. 2011;58:740–8.
83. Fukushima K, Javadi MS, Higuchi T, Lautamaki R, Merrill J, Nekolla SG, et al. Prediction of short-term cardiovascular events using quantification of global myocardial flow reserve in patients referred for clinical 82Rb PET perfusion imaging. J Nucl Med. 2011;52:726–32.
84. Hachamovitch R, Hayes SW, Friedman JD, Cohen I, Berman DS. Comparison of the short-term survival benefit associated with revascularization compared with medical therapy in patients with no

prior coronary artery disease undergoing stress myocardial perfusion single photon emission computed tomography. Circulation. 2003;107:2900–7.

85. Hachamovitch R, Rozanski A, Hayes SW, Thomson LE, Germano G, Friedman JD, et al. Predicting therapeutic benefit from myocardial revascularization procedures: are measurements of both resting left ventricular ejection fraction and stress-induced myocardial ischemia necessary? J Nucl Cardiol. 2006;13:768–78.
86. Hachamovitch R, Rozanski A, Shaw LJ, Stone GW, Thomson LE, Friedman JD, et al. Impact of ischaemia and scar on the therapeutic benefit derived from myocardial revascularization vs. medical therapy among patients undergoing stress-rest myocardial perfusion scintigraphy. Eur Heart J. 2011;32:1012–24.
87.• Shaw LJ, Berman DS, Picard MH, Friedrich MG, Kwong RY, Stone GW, et al. Comparative definitions for moderate-severe ischemia in stress nuclear, echocardiography, and magnetic resonance imaging. JACC Cardiovasc Imaging. 2014;7:593–604. **State-of-the-art paper on the comparative definitions of moderate-severe ischemia in stress nuclear, echocardiography and magnetic resonance imaging**.
88.•• Windecker S, Kolh P, Alfonso F, Collet JP, Cremer J, Falk V. 2014 ESC/EACTS Guidelines on myocardial revascularization: The Task Force on Myocardial Revascularization of the European Society of Cardiology (ESC) and the European Association for Cardio-Thoracic Surgery (EACTS) developed with the special contribution of the European Association of Percutaneous Cardiovascular Interventions (EAPCI). Eur Heart J. 2014;35(et al):2541–619. **Current European guidelines on coronary revascularization therapy**.
89. Patel MR, Dehmer GJ, Hirshfeld JW, Smith PK, Spertus JA. ACCF/SCAI/STS/AATS/AHA/ASNC/HFSA/SCCT 2012 appropriate use criteria for coronary revascularization focused update: a report of the American College of Cardiology Foundation Appropriate Use Criteria Task Force, Society for Cardiovascular Angiography and Interventions, Society of Thoracic Surgeons, American Association for Thoracic Surgery, American Heart Association, American Society of Nuclear Cardiology, and the Society of Cardiovascular Computed Tomography. J Am Coll Cardiol. 2012;59:857–81.
90. Tillisch J, Brunken R, Marshall R, Schwaiger M, Mandelkern M, Phelps M, et al. Reversibility of cardiac wall-motion abnormalities predicted by positron tomography. N Engl J Med. 1986;314:884–8.
91. Beanlands RS, Ruddy TD, deKemp RA, Iwanochko RM, Coates G, Freeman M, et al. Positron emission tomography and recovery following revascularization (PARR-1): the importance of scar and the development of a prediction rule for the degree of recovery of left ventricular function. J Am Coll Cardiol. 2002;40:1735–43.
92. Beanlands RS, Nichol G, Huszti E, Humen D, Racine N, Freeman M, et al. F-18-fluorodeoxyglucose positron emission tomography imaging-assisted management of patients with severe left ventricular dysfunction and suspected coronary disease: a randomized, controlled trial (PARR-2). J Am Coll Cardiol. 2007;50:2002–12.
93. Tamaki N, Yonekura Y, Yamashita K, Saji H, Magata Y, Senda M, et al. Positron emission tomography using fluorine-18 deoxyglucose in evaluation of coronary artery bypass grafting. Am J Cardiol. 1989;64:860–5.
94. vom Dahl J, Eitzman DT, al-Aouar ZR, Kanter HL, Hicks RJ, Deeb GM, et al. Relation of regional function, perfusion, and metabolism in patients with advanced coronary artery disease undergoing surgical revascularization. Circulation. 1994;90:2356–66.
95. Di Carli MF, Davidson M, Little R, Khanna S, Mody FV, Brunken RC, et al. Value of metabolic imaging with positron emission tomography for evaluating prognosis in patients with coronary artery disease and left ventricular dysfunction. Am J Cardiol. 1994;73:527–33.
96. D'Egidio G, Nichol G, Williams KA, Guo A, Garrard L, deKemp R, et al. Increasing benefit from revascularization is associated with increasing amounts of myocardial hibernation: a substudy of the PARR-2 trial. JACC Cardiovasc Imaging. 2009;2:1060–8.
97. Inaba Y, Chen JA, Bergmann SR. Quantity of viable myocardium required to improve survival with revascularization in patients with ischemic cardiomyopathy: a meta-analysis. J Nucl Cardiol. 2010;17:646–54.
98. Birnie D, de Kemp RA, Tang AS, Ruddy TD, Gollob MH, Guo A, et al. Reduced septal glucose metabolism predicts response to cardiac resynchronization therapy. J Nucl Cardiol. 2012;19:73–83.
99. Schinkel AF, Bax JJ, Poldermans D, Elhendy A, Ferrari R, Rahimtoola SH. Hibernating myocardium: diagnosis and patient outcomes. Curr Probl Cardiol. 2007;32:375–410.
100. Underwood SR, de Bondt P, Flotats A, Marcasa C, Pinto F, Schaefer W, et al. The current and future status of nuclear cardiology: a consensus report. Eur Heart J Cardiovasc Imaging. 2014;15:949–55.
101. Beanlands RS, Hendry PJ, Masters RG, deKemp RA, Woodend K, Ruddy TD. Delay in revascularization is associated with increased mortality rate in patients with severe left ventricular dysfunction and viable myocardium on fluorine 18-fluorodeoxyglucose positron emission tomography imaging. Circulation. 1998;98:II51–6.
102. Tarakji KG, Brunken R, McCarthy PM, Al-Chekakie MO, Abdel-Latif A, Pothier CE, et al. Myocardial viability testing and the effect of early intervention in patients with advanced left ventricular systolic dysfunction. Circulation. 2006;113:230–7.
103. Abraham A, Nichol G, Williams KA, Guo A, deKemp RA, Garrard L, et al. 18F-FDG PET imaging of myocardial viability in an experienced center with access to 18F-FDG and integration with clinical management teams: the Ottawa-FIVE substudy of the PARR 2 trial. J Nucl Med. 2010;51:567–74.
104. Sasano T, Abraham MR, Chang KC, Ashikaga H, Mills KJ, Holt DP, et al. Abnormal sympathetic innervation of viable myocardium and the substrate of ventricular tachycardia after myocardial infarction. J Am Coll Cardiol. 2008;51:2266–75.
105. Fallavollita JA, Heavey BM, Luisi Jr AJ, Michalek SM, Baldwa S, Mashtare Jr TL, et al. Regional myocardial sympathetic denervation predicts the risk of sudden cardiac arrest in ischemic cardiomyopathy. J Am Coll Cardiol. 2014;63:141–9.
106. Rudd JH, Warburton EA, Fryer TD, Jones HA, Clark JC, Antoun N, et al. Imaging atherosclerotic plaque inflammation with [18F]-fluorodeoxyglucose positron emission tomography. Circulation. 2002;105:2708–11.
107. Joshi NV, Vesey AT, Williams MC, Shah AS, Calvert PA, Craighead FH, et al. 18F-fluoride positron emission tomography for identification of ruptured and high-risk coronary atherosclerotic plaques: a prospective clinical trial. Lancet. 2014;383:705–13.
108. Erba PA, Sollini M, Lazzeri E, Mariani G. FDG-PET in cardiac infections. Semin Nucl Med. 2013;43:377–95.
109. Hiari N, Rudd JH. FDG PET imaging and cardiovascular inflammation. Curr Cardiol Rep. 2011;13:43–8.
110. Millar BC, Prendergast BD, Alavi A, Moore JE. 18FDG-positron emission tomography (PET) has a role to play in the diagnosis and therapy of infective endocarditis and cardiac device infection. Int J Cardiol. 2013;167:1724–36.
111.• Bruun NE, Habib G, Thuny F, Sogaard P. Cardiac imaging in infectious endocarditis. Eur Heart J. 2014;35:624–32. **Overview of the different non-invasive imaging modalities in the diagnosis of infectious endocarditis**.

112. Sobic-Saranovic D, Artiko V, Obradovic V. FDG PET imaging in sarcoidosis. Semin Nucl Med. 2013;43:404–11.

113.• Schatka I, Bengel FM. Advanced imaging of cardiac sarcoidosis. J Nucl Med. 2014;55:99–106. **Overview of the clinical usefulness of ^{18}F-FDG PET in cardiac sarcoidosis in relation to other imaging modalities**.

114. Skali H, Schulman AR, Dorbala S. 18F-FDG PET/CT for the assessment of myocardial sarcoidosis. Curr Cardiol Rep. 2013;15:352.

115. Hamzeh NY, Wamboldt FS, Weinberger HD. Management of cardiac sarcoidosis in the United States: a Delphi study. Chest. 2012;141:154–62.

116.•• Birnie DH, Sauer WH, Bogun F, Cooper JM, Culver DA, Duvernoy CS, et al. HRS expert consensus statement on the diagnosis and management of arrhythmias associated with cardiac sarcoidosis. Heart Rhythm. 2014;11:1305–23. **Consensus document on the diagnosis and clinical management of arrhythmias associated with cardiac sarcoidosis**.

117. Youssef G, Leung E, Mylonas I, Nery P, Williams K, Wisenberg G, et al. The use of 18F-FDG PET in the diagnosis of cardiac sarcoidosis: a systematic review and metaanalysis including the Ontario experience. J Nucl Med. 2012;53:241–8.

118. Tahara N, Tahara A, Nitta Y, Kodama N, Mizoguchi M, Kaida H, et al. Heterogeneous myocardial FDG uptake and the disease activity in cardiac sarcoidosis. JACC Cardiovasc Imaging. 2010;3:1219–28.

119.• Blankstein R, Osborne M, Naya M, Waller A, Kim CK, Murthy VL, et al. Cardiac positron emission tomography enhances prognostic assessments of patients with suspected cardiac sarcoidosis. J Am Coll Cardiol. 2014;63:329–36. **First study to report the relation between cardiac PET findings and clinical outcome in patients with cardiac sarcoidosis**.

120. Saby L, Le Dolley Y, Laas O, Tessonnier L, Cammilleri S, Casalta JP, et al. Early diagnosis of abscess in aortic bioprosthetic valve by 18F-fluorodeoxyglucose positron emission tomography-computed tomography. Circulation. 2012;126:e217–20.

121. Ploux S, Riviere A, Amraoui S, Whinnett Z, Barandon L, Lafitte S, et al. Positron emission tomography in patients with suspected pacing system infections may play a critical role in difficult cases. Heart Rhythm. 2011;8:1478–81.

122. Bensimhon L, Lavergne T, Hugonnet F, Mainardi JL, Latremouille C, Maunoury C, et al. Whole body [(18) F]fluorodeoxyglucose positron emission tomography imaging for the diagnosis of pacemaker or implantable cardioverter defibrillator infection: a preliminary prospective study. Clin Microbiol Infect. 2011;17:836–44.

123. Sarrazin JF, Philippon F, Tessier M, Guimond J, Molin F, Champagne J, et al. Usefulness of fluorine-18 positron emission tomography/computed tomography for identification of cardiovascular implantable electronic device infections. J Am Coll Cardiol. 2012;59:1616–25.

124. Tlili G, Amroui S, Mesguich C, Riviere A, Bordachar P, Hindie E, et al. High performances of (18)F-fluorodeoxyglucose PET-CT in cardiac implantable device infections: a study of 40 patients. J Nucl Cardiol. 2015;22:787–98.

125. Saby L, Laas O, Habib G, Cammilleri S, Mancini J, Tessonnier L, et al. Positron emission tomography/computed tomography for diagnosis of prosthetic valve endocarditis: increased valvular 18F-fluorodeoxyglucose uptake as a novel major criterion. J Am Coll Cardiol. 2013;61:2374–82.

126. Patterson RE, Eisner RL, Horowitz SF. Comparison of cost-effectiveness and utility of exercise ECG, single photon emission computed tomography, positron emission tomography, and coronary angiography for diagnosis of coronary artery disease. Circulation. 1995;91:54–65.

127. Gould KL, Goldstein RA, Mullani NA. Economic analysis of clinical positron emission tomography of the heart with rubidium-82. J Nucl Med. 1989;30:707–17.

128. Merhige ME, Breen WJ, Shelton V, Houston T, D'Arcy BJ, Perna AF. Impact of myocardial perfusion imaging with PET and (82)Rb on downstream invasive procedure utilization, costs, and outcomes in coronary disease management. J Nucl Med. 2007;48:1069–76.

129. Beanlands RS, deKemp RA, Smith S, Johansen H, Ruddy TD. F-18-fluorodeoxyglucose PET imaging alters clinical decision making in patients with impaired ventricular function. Am J Cardiol. 1997;79:1092–5.

130. Jacklin PB, Barrington SF, Roxburgh JC, Jackson G, Sariklis D, West PA, et al. Cost-effectiveness of preoperative positron emission tomography in ischemic heart disease. Ann Thorac Surg. 2002;73:1403–10.